Influence of Extracellular Monovalent Cations on Pore and Gating Properties of $P2X_7$ Receptor-Operated Single-Channel Currents

T. Riedel,* G. Schmalzing,† and F. Markwardt*
*Julius-Bernstein-Institute for Physiology, Martin Luther University Halle, Halle/Saale, Germany; and †RWTH Aachen University, Department of Molecular Pharmacology, Aachen, Germany

ABSTRACT Using the patch-clamp method, we studied the influence of external alkali and organic monovalent cations on the single-channel properties of the adenosine triphosphate (ATP)-activated recombinant human $P2X_7$ receptor. The slope conductance of the $hP2X_7$ channel decreased and the reversal potential was shifted to more negative values as the ionic diameter of the organic test cations increased. From the relationship between single-channel conductance and the dimensions of the inward current carrier, the narrowest portion of the pore was estimated to have a mean diameter of ~8.5 Å. Single-channel kinetics and permeation properties remained unchanged during receptor activation by up to 1 mM ATP^{4-} for >1 min, arguing against a molecular correlate of pore dilation at the single $P2X_7$ channel level. Substitution of extracellular Na^+ by any other alkali or organic cation drastically increased the open probability of the channels by prolonging the mean open time. This effect seems to be mediated allosterically through an extracellular voltage-dependent Na^+ binding site with a K_d of ~5 mM Na^+ at a membrane potential of −120 mV. The modulation of the ATP-induced $hP2X_7$ receptor gating by extracellular Na^+ could be well described by altering the rate constant from the open to the neighboring closed state in a C-C-C-O kinetic receptor model. We suggest that $P2X_7$ receptor-induced depolarization and associated K^+-efflux may reduce Na^+ occupancy of the regulatory Na^+ binding site and thus increase the efficacy of ATP^{4-} in a feed-forward manner in $P2X_7$ receptor-expressing cells.

INTRODUCTION

The $P2X_7$ receptor belongs to the seven-member P2X gene family, which encodes membrane glycoproteins that function as trimeric adenosine triphosphate (ATP)-gated cation channels in the plasma membrane of a large variety of cells throughout the body. $P2X_7$ receptors are primarily expressed in epithelial cells and antigen-presenting cells such as lymphocytes, mast cells, and macrophages, where they seem to exert immunomodulatory functions including inflammatory cytokine release, membrane fusion events, and apoptosis (for a recent review, see (1)). Like other P2X receptor subtypes, $P2X_7$ receptors respond to brief (≤1 s) stimulation with extracellular ATP by the fast opening of an intrinsic cation-conducting pore, permitting the selective permeation of small cations (Na^+, K^+, and Ca^{2+}) into the cell. As a result, the plasma membrane depolarizes and the Na^+ and K^+ gradients collapse. A particular feature of $P2X_7$ receptors is that prolonged or repeated activation by ATP promotes the formation of large pores; these pores allow the bidirectional passage of molecules into the cell, as indicated by the entry of organic cations of up to 900 Da, and the leakage of metabolites (2). If ATP activation is sustained for >15–30 min, permeabilization becomes irreversible in most cell types and cells start to lyse or undergo apoptosis (1).

The mechanism for large pore formation has not been unequivocally clarified thus far. For several years, the idea has been promoted, supported by experimental data, that $P2X_7$ receptors (and in a similar manner also $P2X_2$ and $P2X_4$ receptors) are capable of progressively increasing the diameter of the initially Na^+, K^+, and Ca^{2+}-selective pathway to accommodate larger and larger molecules (for reviews see (2,3)). This phenomenon has been designated ''pore dilatation.'' However, there is also early indication from experiments with the marine toxin maitotoxin that the lytic pore and the $P2X_7$ receptor may constitute separate entities (4). Recently, the possibility of separate entities gained further strong support from studies suggesting that the $P2X_7$ receptor-dependent permeabilization to large molecules involves a modulation of the multidrug transporter P-glycoprotein (5) or recruitment of pannexin-1, a connexin-like hemichannel (6). Additionally, our single $P2X_7$ channel experiments (7) revealed that the apparent pore dilatation of $P2X_7$ receptors observed in macroscopic current recordings (8,9) has no equivalent at the single-channel level, suggesting also that the $P2X_7$ receptor-induced permeability increase is secondary to $P2X_7$ receptor activation.

If the lytic properties of $P2X_7$ receptors are mediated through the activation of cell-type-specific secondary channel structures, then the biophysical and pharmacological properties of the genuine $P2X_7$-receptor channel cannot be reliably inferred from macroscopic measurements. Methods measuring global ATP-induced $P2X_7$ receptor-dependent signals such as whole-cell current recordings, ion fluxes, or changes of intracellular-concentration permeable ions, do not allow a clear discrimination between genuine $P2X_7$

Submitted December 22, 2006, and accepted for publication March 23, 2007.

Address reprint requests to F. Markwardt, Julius-Bernstein Institute for Physiology, Martin Luther University Halle, Magdeburger Str. 6, D-06097 Halle/Saale, Germany. Tel.: 49-345-557-1390; Fax.: 49-345-552-7899; E-mail: fritz.markwardt@medizin.uni-halle.de.

Editor: Tzyh-Chang Hwang.

0006-3495/07/08/846/13 $2.00

doi: 10.1529/biophysj.106.103614

receptor-dependent currents and secondary activated permeation pathways. To overcome these obstacles, we used the patch-clamp method to characterize genuine $P2X_7$ receptor-mediated currents at the single-molecule level. We used inorganic and organic cations to explore the dimension of the narrow portion of the recombinant $hP2X_7$ receptor channel, including a potential change in the channel diameter during prolonged activation by ATP. A dramatic change in the $P2X_7$ receptor single-channel kinetics in Na^+-free bath solutions prompted us to study the influence of extracellular cations on the permeation and kinetic behavior of the $P2X_7$ receptor in greater detail. We found that the pore diameter of single $P2X_7$ channels stays constant during sustained activation by ATP and that extracellular Na^+ strongly favors closure of the $P2X_7$ receptor channel.

MATERIALS AND METHODS

Chemicals

Organic cations, and all other chemicals not otherwise specified were obtained from Sigma (Deisenhofen, Germany). Na_2ATP was purchased from Roche (Mannheim, Germany).

Single-channel patch-clamp electrophysiology on recombinant $P2X_7$ receptors

Microelectrodes were pulled from borosilicate glass, coated with Sylgard (Dow Corning, Midland, MI), and filled with K^+ pipette solution consisting of (in mM) 90 aspartic acid, 10 KCl, 10 EGTA, 10 BAPTA, 10 Hepes, and 0.5 $MgCl_2$, with pH adjusted to 7.2 with KOH. The Cs^+ pipette solution had the same composition except that CsCl and CsOH replaced KCl and KOH, respectively. The pipette resistance was in the range 6–15 MΩ. Electrode potentials were compensated electronically by the patch-clamp amplifier (Axopatch 1D, Axon Instruments, Foster City, CA). The diffusion potential between the Barth's medium and the pipette solution at the tip of the pipette was determined as 3 mV and 5 mV for the K^+ and Cs^+ pipette solutions, respectively, using an established procedure (10). Holding potentials (V_h) and reversal potentials (V_{rev}) were not corrected for tip potentials.

The human $P2X_7$ ($hP2X_7$) receptor was expressed in collagenase-defolliculated *Xenopus laevis* oocytes of stages V and VI by injection of 20 nl (~2 ng/oocyte) of complementary RNA, as described previously (7). Injected oocytes were maintained in petri dishes at 19°C in modified Barth's medium consisting of (in mM) 100 NaCl, 1 KCl, 1 $CaCl_2$, 1 $MgCl_2$, 5 Hepes-NaOH, pH 7.4, supplemented with 10,000 U/ml of penicillin and 10 mg/ml streptomycin. One to three days after injection, experiments were performed on outside-out oocyte patches at room temperature (≈22°C). To this end, the vitelline layer was mechanically removed after a short exposure to a hyperosmotic shrinking solution. Single denuded oocytes were placed in the reference-bath electrode-containing part of a two-part perfusion chamber, and were continuously superfused with Barth's medium without antibiotics. Outside-out patches of the oocyte plasma membrane were pulled within this part of the perfusion chamber.

Once excised, membrane patches were transferred to an electrically connected subcompartment of the perfusion chamber, the bathing solution of which could be exchanged completely within ~3 s. The various bathing solutions used consisted of (mM) 100 X, 0.5 $CaCl_2$, 5 Hepes-Tris, pH 7.4, with X representing the chloride salt of any one of the following cations: Li^+, Na^+, K^+, Cs^+, monomethylammonium$^+$ ($1MA^+$), dimethylammonium$^+$ ($2MA^+$), trimethylammonium$^+$ ($3MA^+$), tetramethylammonium$^+$ ($4MA^+$), tris-(hydroxymethyl)-aminomethane$^+$ ($Tris^+$), N-methyl-D-glucamine$^+$ ($NMDG^+$), or tetraethylammonium$^+$ ($4EA^+$). Fast and reproducible solution change at the outer side of the patch, from ATP-free bathing solution to ATP^{4-}-containing solution of otherwise identical composition, was achieved in <1 ms using a liquid filament switch (7). Free ATP^{4-} concentrations indicated in the figures and in the text were adjusted by varying the total concentrations of ATP and $CaCl_2$, on the basis of the equilibrium dissociation constant of Ca-ATP, in such a way that the free Ca^{2+} concentration was kept constant at 0.5 mM (11). The stability constants for $Tris^+$ were used to calculate the binding of the organic cations to ATP (11). The total concentrations of $CaCl_2$ and ATP used to adjust the ATP^{4-} concentrations indicated in the figures were calculated according to Schubert (11) and are shown in Table 1.

As detailed previously (7), ATP^{4-}-induced currents recorded from outside-out patches of $hP2X_7$ receptor-expressing oocytes consist of two components: 1), typical patterns of inward single-channel events; and 2), a smooth inward shift of the holding current with an exponential time course of activation and deactivation during ATP^{4-} application and withdrawal, respectively. This second component is also observed in patches lacking $hP2X_7$ receptors and most likely represents a nonspecific effect of ATP^{4-} on the patch membrane and the pipette (7). For evaluation of $P2X_7$ receptor-dependent single-channel kinetics, measurements of single-channel current amplitudes or dwell times started 1 s after application of ATP^{4-}, and the steady state or slowly increasing components of the smooth current component were subtracted by the software used.

Currents were recorded and filtered at 1 kHz (if not otherwise stated) using the four-pole Bessel filter of the amplifier and sampled at 5 kHz. Sample-trace data lasting 0.4–4 s were stored and analyzed on a personal computer using software programmed in our department (Superpatch 2000, SP-Analyzer, T. Böhm, University Halle) and the computer program ASCD (generously provided by G. Droogmans, Catholic University, Leuven, Belgium) using least-square algorithms for fitting amplitude and dwell-time histograms.

Channel open probabilities (P_o) were calculated from the amplitude histogram. Only patches with no more than three overlapping single-channel events were used. The number of channels in a patch was assumed to correspond to the maximal number of overlapping events at an activating ATP^{4-} concentration of 1 mM, where P_o is high. In cases of more than one

TABLE 1 Calculated ATP^{4-} concentrations in $CaCl_2$-containing extracellular solutions

$[ATP^{4-}]$ (mM)	$[ATP]_{abs}$ (mM)	$[Ca^{2+}]_{abs}$ (mM)	Monovalent cation
10	57	34.7	Na
3	17	10.8	Na
1	5.7	3.95	Na
0.3	1.7	1.53	Na
0.1	0.57	0.85	Na
0.03	0.17	0.6	Na
0.01	0.057	0.53	Na
0.003	0.017	0.51	Na
10	52.03	34.7	K
3	15.8	10.8	K
1	5.3	3.95	K
0.3	1.6	1.53	K
0.1	0.53	0.845	K
0.03	0.16	0.6	K
0.01	0.053	0.53	K
0.003	0.016	0.51	K
0.1	1.3	0.85	Li
0.1	0.5	0.85	Cs
1	5.2	3.95	organic
0.1	0.52	0.85	organic

The absolute concentrations of $CaCl_2$ and ATP needed to achieve the desired concentration of ATP^{4-} at 0.5 mM constant free Ca^{2+} were calculated according to Schubert (11).

active channel in the patch, an equal P_o for all these channels was assumed, and the mean P_o was calculated by the following binomial distribution

$$P_o = 1 - \sqrt[n]{P(0)}, \quad (1)$$

where n is the number of active channels in the patch, and $P(0)$ is the closed probability derived from the fit of the amplitude histogram.

For calculation of dwell-time histograms, only apparent single-channel patches (as judged by the absence of overlapping openings at maximal open probabilities) were used. The detection threshold for opening and closing was set at 50% of the single-channel current amplitude.

Diameters of dehydrated alkali cations of 1.20, 1.90, 2.66, and 3.38 Å, increasing from Li^+ to Na^+ to K^+ to Cs^+, were taken from published data (12). Effective diameters of organic cations, which are shown in Supplementary Material 1, were calculated as the smallest possible diameter of a circular pore allowing permeation of the molecule, using the freeware program ArgusLab 4.0.1 (Mark A. Thompson, Planaria Software, Seattle, WA, http://www.arguslab.com).

Averaged data are given as mean ± SD of N measurements unless otherwise stated. The statistical significance ($P < 0.05$) of differences between means was assessed by one-way ANOVA followed by Bonferroni's multiple-comparison t-test using Jandel Sigmastat statistical software (SPSS, Chicago, IL). The Sigmaplot program (SPSS) was used for function fitting and graphical presentation of the data. Theoretical values for dwell times, open probabilities, and relaxation time constants were derived by simulation using the freely accessible program SCALCS (http://www.ucl.ac.uk/Pharmacology/dc.html) (13).

RESULTS

Single hP2X$_7$ receptors display apparently only one gating mode in Na^+-free solutions

In Na^+-based extracellular solutions, P2X$_7$ receptor-operated channel openings exhibited a dual mode of gating with short- and long-lasting open states (7). Although the short openings were consistently observed, the long openings appeared particularly at high ATP^{4-} concentrations. Circumstantial evidence suggested that the transitions between short and long openings reflect a modal gating behavior of the hP2X$_7$ receptor rather than a change in the permeation characteristics to cations. Because of the large increase of the mean open probability and open time in Na^+-free extracellular solutions, the two gating modes could not be resolved in solutions in which Na^+ was replaced by other cations. For the analysis of currents recorded in Na^+ solution, we used only patches displaying short openings. Accordingly, only one value is given for each parameter in this work.

Determination of the effective pore radius of the hP2X$_7$ receptor channel

To probe the permeation pathway of the hP2X$_7$ receptor, we examined the conductance of a series of alkali and organic cations of increasing diameter ranging from 1.2 Å (Li^+) to 8.3 Å ($4EA^+$). The hP2X$_7$ channel was opened with 0.1 or 1 mM extracellular ATP^{4-}. Reversal potential measurements were done under bi-ionic conditions with one of the organic test cations and Cs^+ in the extracellular bath and patch pipette solutions, respectively. Accordingly, inward currents were expected to be carried by the test cation present at the extracellular side of the membrane, whereas outward currents were expected to be essentially carried by Cs^+ at the cytoplasmic side of the membrane.

Fig. 1 shows typical recordings of ATP^{4-}-induced single-channel currents in response to voltage ramps for Na^+ (the most permeant cation tested, see Fig. 2 *A*) and four methylated NH_4^+ derivatives. Inwardly-directed single-channel currents were observed at negative potentials, indicating that the hP2X$_7$ receptor is permeable to all of the four organic cations tested. In the Na^+-based solution, single-channel conductance became larger at negative potentials, indicating a weak inward rectification (Fig. 1 *B*) similar to hP2X$_7$ receptor-mediated whole-cell currents recorded under analogous conditions from human B lymphocytes (14) and *X. laevis* oocytes (15). Inward rectification has also been commonly observed with P2X$_2$ receptors at both the whole-cell and single-channel levels (16), where it has been attributed to binding of the permeating Na^+ to a site in the channel pore within the electrical field of the membrane. Fig. 1, *C–F*, shows that inward rectification was reduced when extracellular Na^+ was replaced by one of the large organic cations, for reasons that were not further investigated.

With increasing diameter of the cations, the single-channel conductance successively decreased and the reversal potential was shifted toward more negative values. Reversal potentials and slope conductances were calculated by linear regression of single-channel amplitude versus patch membrane potential 50 mV above and below the respective reversal potential. An increase of the cation diameter from 1.9 Å (Na^+) to 6.7 Å ($4MA^+$) was associated with a decrease of the slope conductance from 10.6 pS to 2.3 pS and an average increase of the reversal potential from −8.3 mV to −78.2 mV (Fig. 1, *B* and *F*). A similar decrease in slope conductance (Fig. 2 *A*) and increase of reversal potential (Fig. 2 *B*) as observed with $4MA^+$ was also seen when Na^+ was replaced by other large organic cations of similar size, such as $Tris^+$, $NMDG^+$, or TEA^+. The permeability sequence suggested that the hP2X$_7$ receptor distinguishes various permeant organic cations predominantly by their size. An effective diameter of the P2X$_7$ channel pore of ~8.5 Å was obtained by plotting the single-channel conductance versus the apparent molecular diameter of the current carrier and extrapolating the diameter to $\gamma = 0$ (Fig. 2 *C*).

Although P2X$_7$ channels are permeable for Ca^{2+} and the solutions contained 0.5 mM free Ca^{2+}, a substantial contribution of Ca^{2+} fluxes to the measured permeation characteristics seems unlikely for the following reasons: 1), At the whole cell level (V_h −55 mV), Egan and Khakh (17) determined a relative contribution of 4.6% of Ca^{2+} to the P2X$_7$ receptor-operated current in extracellular solutions containing 145 mM Na^+, 1 mM Mg^{2+}, and 2 mM Ca^{2+}. Assuming a linear dependence of the relative Ca^{2+} conductance on the relative concentration of extracellular Ca^{2+} and independence on both the membrane potential and the

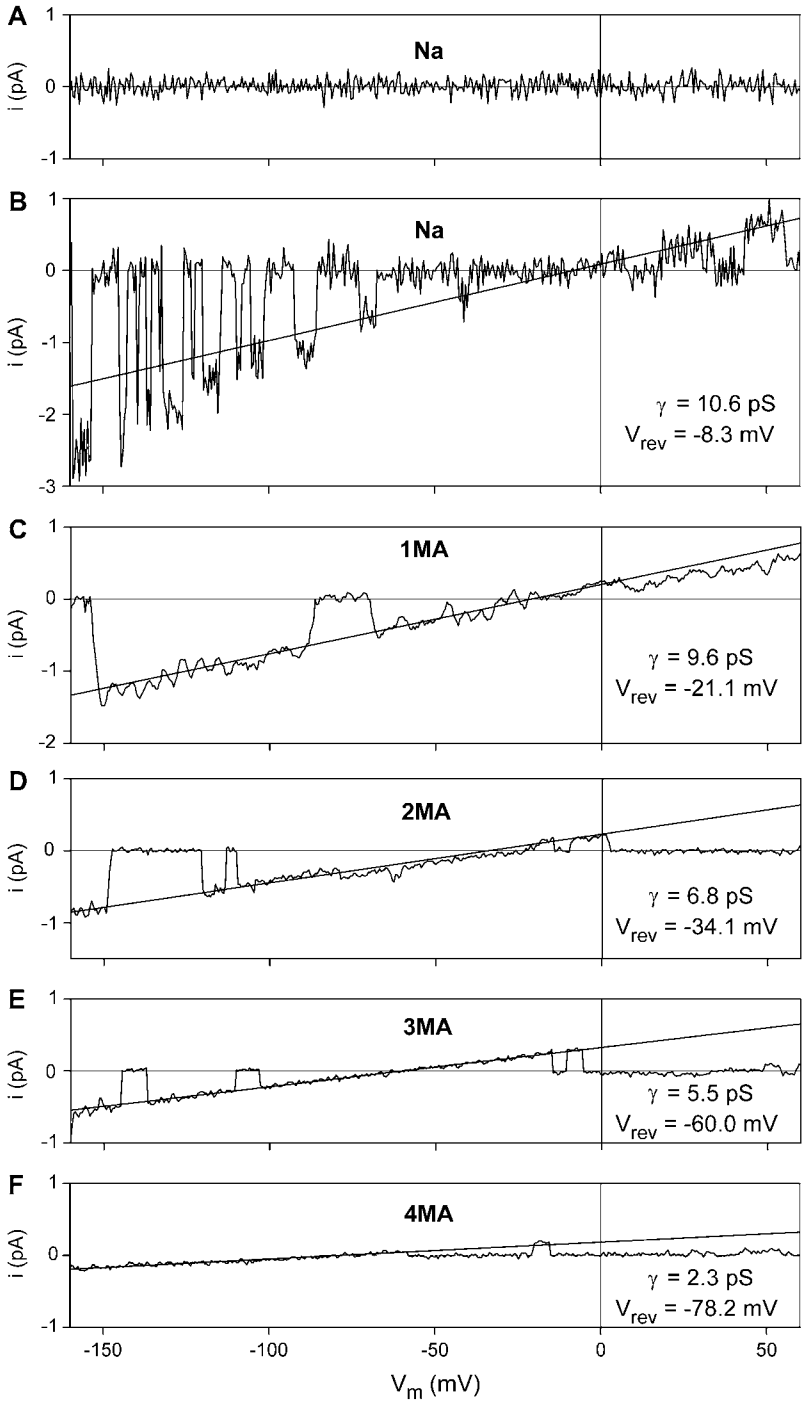

FIGURE 1 Representative single-channel recordings of hP2X$_7$ receptor-mediated currents from outside-out patches exposed to different extracellular cations. The horizontal lines represent zero current when the hP2X$_7$ channel in the patch is closed. Downward and upward deflections correspond to channel openings at negative and positive voltages, respectively. Currents were recorded during voltage ramp pulses extending from −160 to +60 mV within 1 s before (*A*) and during (*B–F*) hP2X$_7$ receptor activation by 1 mM ATP^{4-} in extracellular solutions with the main monovalent cation in the bath as indicated. Leak currents and non-specific ATP^{4-}-induced currents (for details, see (7) were subtracted. To demonstrate the current-voltage relationship of P2X$_7$ receptor-operated channels despite the low mean open probability in Na^+ solution, a current trace displaying nonrepresentative high open probability is shown in *B*. Straight lines represent a linear fit of the open channel current against voltage ramp ranging from −50 to +50 mV below and above the respective reversal potential V_{rev}. Current signals were filtered at 1000 Hz (*A* and *B*) or 100 Hz (*C–F*). The Cs^+ pipette solution was used. The values derived for slope conductance γ and V_{rev} are indicated in the graph.

particular monovalent cation species present, the fractional current carried by Ca^{2+} under our conditions (100 mM monovalent, 0.5 mM Ca^{2+}) can be estimated to be ~1.7%. Taking this value and the mean conductance in Na^+-based extracellular solutions of ~11 pS into account, a fractional Ca^{2+} conductance of ~0.18 pS is derived, which is far below the 2–3 pS measured for the largest organic cations tested, suggesting that the contribution of Ca^{2+} is negligible.

2) In a few preliminary measurements ($N = 2$ to 3 patches), we examined the effect of the extracellular Ca^{2+} concentrations on the conductance γ and the reversal potential V_{rev} of P2X$_7$ receptor-operated single-channel currents in 100 mM $NMDG^+$-based extracellular solution. No significant changes were found at 0.2, 0.5, and 2 mM free extracellular Ca^{2+}, at which γ values (V_{rev} values) of 2.6 ± 0.3 pS (−74.4 ± 5.8 mV), 2.9 ± 0.2 pS (−74.7 ± 3.8 mV) and 2.6 ± 0.3 pS

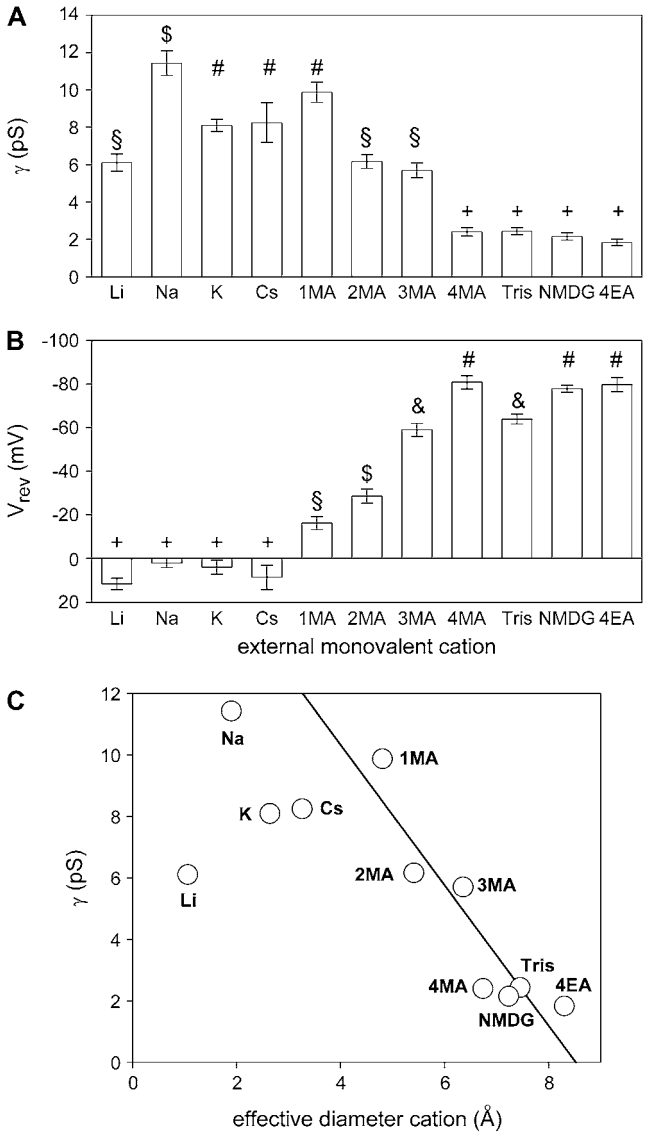

FIGURE 2 Slope conductance and reversal potential of ATP-activated $P2X_7$ receptor channels for each extracellular cation tested. Statistical comparisons were made between (*A*) single-channel conductances or (*B*) reversal potentials recorded under asymmetric conditions (Cs^+ pipette solution) from outside-out patches exposed to different extracellular cations. Data were obtained as shown in Fig. 1 and are given as mean ± SE of 3–15 independent measurements. Means labeled with different letters are significantly differ from one another. (*C*) Slope conductance γ of single $hP2X_7$ channels versus the ionic diameter of each cation. A minimal effective diameter of the $hP2X_7$ receptor channel of 8.5 ± 0.4 Å was derived by extrapolating the linear regression fit of the values for the organic cations, shown as a solid line, to zero conductance.

(−68.9 ± 3.9 mV) were measured, respectively (mean ± SE). Accordingly, we think that a correction of the data analysis for Ca^{2+} permeability is unnecessary. Only at 10 mM Ca^{2+} was a significant positive shift in the reversal potential observed ($\gamma = 3.1 \pm 0.4$ pS, $V_{rev} = -54.4 \pm 6.7$ mV), as compared to the Ca^{2+}-free solution.

Replacing external Na^+ by other monovalent cations increases the single-channel open probability

Fig. 3 demonstrates typical examples of ATP^{4-}-induced single-channel currents in bathing solutions with different species of monovalent cations. In addition to the successive decrease of the single-channel amplitude with increasing diameter of the tested organic cation, it is apparent that the open probability and the open times increased dramatically when Na^+ was replaced by one of the indicated cations. The single-channel current amplitude and open probability (as well as the conductance and the reversal potential, data not shown) did not change during sustained channel activation, irrespective of the species of extracellular monovalent cation. As an example, the two lowest panels of Fig. 3 show representative single-channel current traces of 2 s duration recorded in 100 mM $NMDG^+$ 2 s after initiating and just before stopping a 30-s channel activation by 0.1 mM ATP^{4-}. Channel conductance and open probability were fairly constant over the longest time period (30 s) examined.

Similarly, also replacing extracellular Na^+ by K^+ produced markedly prolonged mean channel open times τ_o, from 6 ms to 94 ms, as shown in Fig. 4. In extracellular solutions containing both Na^+ and K^+, an intermediate mean open time of 65 ms was observed (Fig. 4, *middle*). In K^+-based extracellular solutions, both the amplitudes of the single-channel currents (Fig. 5 *A*) and the increased mean open times (Fig. 5 *C*) were independent of the activating ATP^{4-}-concentration ($[ATP^{4-}]$). In contrast, the open probability P_o increased significantly with increasing $[ATP^{4-}]$ (Fig. 5 *B*).

In a C-C-C-O model of channel gating, when all ATP^{4-} binding sites have the same affinity and there is no cooperative interaction between them, the $[ATP^{4-}]$ dependence of the open probability is given by

$$P_o([ATP^{4-}]) = \frac{P_{o,\infty}}{\left(1 + \frac{10^{-\log K_d}}{[ATP^{4-}]}\right)^n}, \qquad (2)$$

where $P_{o,\infty}$ is the maximal open probability at saturating ATP^{4-} concentrations, K_d is the apparent ATP^{4-} dissociation constant, and n is the number of bound ATP^{4-} molecules needed for channel opening. Compared to data obtained in Na^+-based media (7), P_0 was increased in K^+-based media from 0.26 ± 0.02 to 0.86 ± 0.01, and the pK_d-value ($-\log K_d$) was increased from 3.93 ± 0.14 to 4.36 ± 0.09. Only the coefficient n of 1.6 ± 0.2 (mean ± SE) was virtually the same in Na^+ and K^+-based extracellular solutions (7).

The $[ATP^{4-}]$-dependent increase of the open probability resulted from a decrease of the mean closed time τ_c shown in Fig. 5 *D*. The mean closed times measured here were significantly larger in K^+ than in Na^+ media at external $ATP^{4-} < 30\ \mu M$, but not significantly different at $> 30\ \mu M$ ATP^{4-} (7). The reason for this is probably that in (7), traces analyzed for dwell times lasted maximally 0.4 s, limiting the

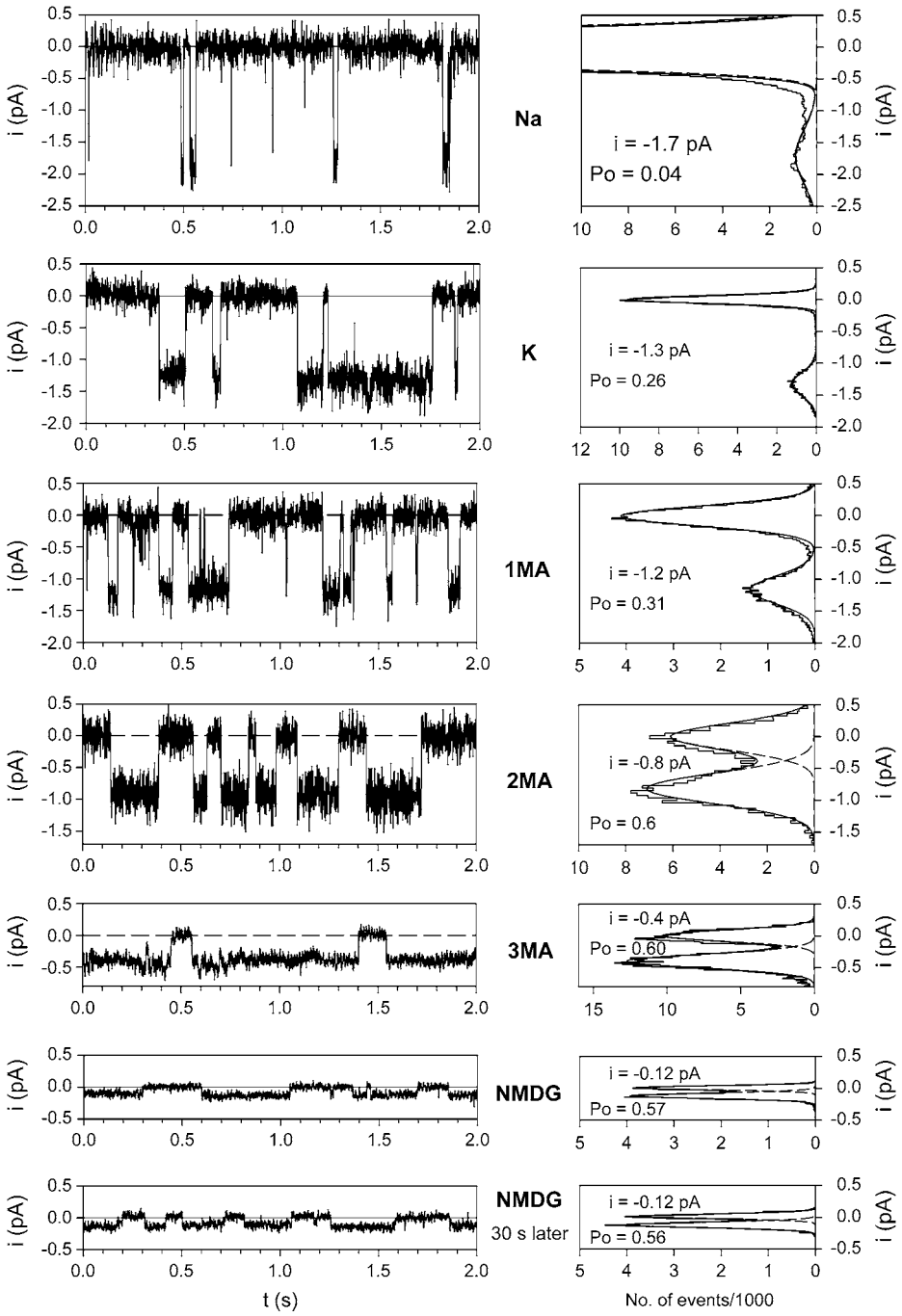

FIGURE 3 Cation-dependent conductance of single P2X$_7$-dependent ion channels. Data shown are representative current traces (*left*) and corresponding amplitude histograms (*right*) after subtraction of the leak and nonspecific ATP^{4-}-induced currents. The two lowermost current traces were recorded 2 s after starting the ATP^{4-}-application or 30 s later, as indicated. Currents were filtered at 1000 Hz (Na^+, K^+, $1MA^+$, and $2MA^+$), 300 Hz ($3MA^+$) or 100 Hz ($NMDG^+$). K^+ pipette solution, $V_h = -140$ mV, $[ATP^{4-}] = 0.1$ mM.

maximally observable closed time duration whereas the traces described here lasted 4 s.

The influence of the extracellular monovalent cations on the single-channel kinetics of the P2X$_7$ receptor is summarized in Fig. 6. The open probability in Na^+ and Cs^+ solutions was significantly lower than in all other cation solutions tested (Fig. 6 *A*). A comparison of mean open times (Fig. 6 *B*) and mean closed times (Fig. 6 *C*) reveals that the mechanisms that determine the low open probabilities of these two alkali cations are fundamentally different. In Na^+ solutions, the low open probability results from an extremely short mean open time that is unique for Na^+ (Fig. 6 *B*), whereas the closed time was not significantly different to any of the other cations tested except Cs^+ (Fig. 6 *C*). Contrarily, the low open probability in Cs^+ solutions is largely determined by a significantly increased mean closed time that is unique for Cs^+ (Fig. 6 *C*). The mean open time in Cs^+ solution, on the other hand, was substantially larger than the mean open time in Na^+ solution; this Cs^+-evoked increase in the mean open time was of similar magnitude as

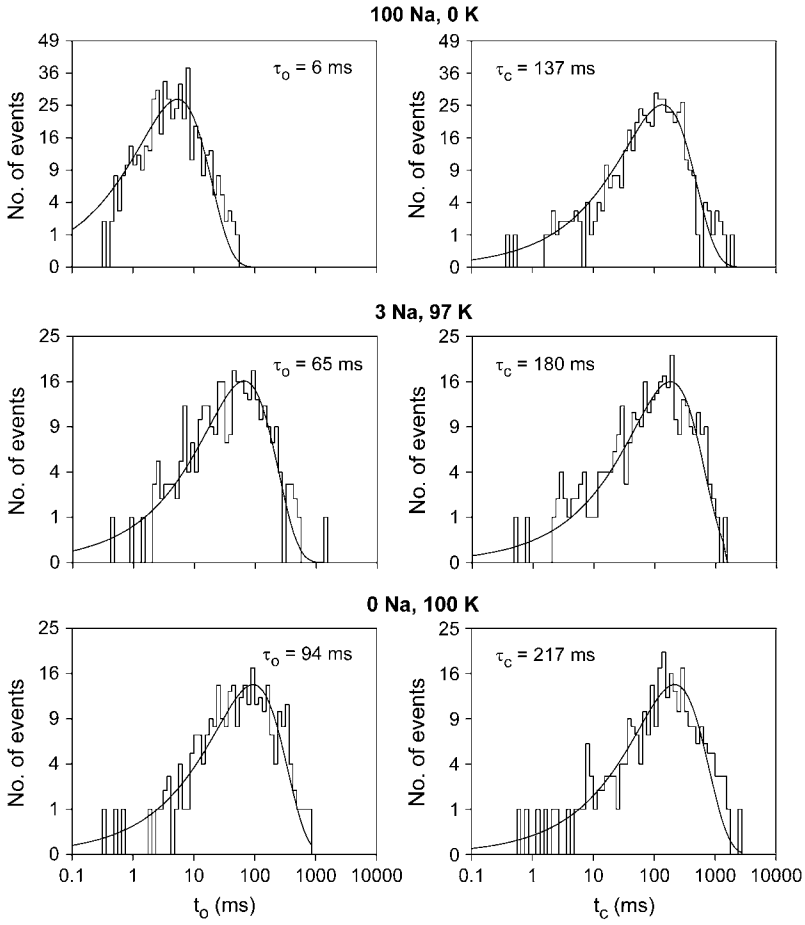

FIGURE 4 Example of the dependence of hP2X$_7$ receptor single-channel kinetics on extracellular Na^+. Shown are typical dwell-time histograms of recordings from a single patch in extracellular solutions consisting of the indicated monovalent cations (in mM). The approximated mean dwell times are indicated. K^+ pipette solution, $V_h = -120$ mV, $[ATP^{4-}] = 0.1$ mM.

that evoked by the other Na^+ substitutes, i.e., K^+ and organic cations.

Replacing external Na^+ by other monovalent cations delayed single-channel closure

Recordings from a patch containing about four hP2X$_7$ receptors showed that the closing of P2X$_7$ receptor single channels on ATP^{4-} withdrawal (deactivation) was drastically delayed when the extracellular cation is $1MA^+$ rather than Na^+ (Fig. 7, *A* and *B*) or any other of the monovalent cations studied (results not shown). To examine the influence of replacing extracellular Na^+ with K^+ on current activation and deactivation at the macroscopic level, responses to several ATP^{4-} applications were recorded using ensemble-averaged current from multichannel patches or patches with few P2X$_7$ receptor channels. The activation time course was approximated by

$$i_{act}(t) = i_{act,\infty,c} \times \left(1 - e^{-\frac{t - t_{del,act}}{\tau_{act,c}}}\right) + i_{act,\infty,s} \times \left(1 - e^{-\frac{t - t_{del,act}}{\tau_{act,s}}}\right) + s \times (t - t_{del,act}) + i_0, \quad (3)$$

where $i_{act,\infty,c}$ and $i_{act,\infty,s}$ are the amplitudes of steady-state currents of the noisy mean single-channel current and a channel-independent unspecific ''smooth'' ATP^{4-}-induced current (7), respectively, after infinite time of ATP^{4-} application. $\tau_{act,c}$ and $\tau_{act,s}$ are the corresponding activation time constants. $t_{del,act}$ is the delay of the onset of the ATP^{4-}-induced current, s is the slope of the linearly increasing part of the unspecific current, and i_0 is the steady-state current in the absence of ATP^{4-}.

The deactivation during fast ATP^{4-} washout was described by:

$$i_{deact}(t) = i_{deact,c} \times e^{-\frac{t - t_{del,deact}}{\tau_{deact,c}}} + i_{deact,s} \times e^{-\frac{t - t_{del,deact}}{\tau_{deact,s}}} + i_0, \quad (4)$$

where i_0 and $t_{del,deact}$ have the same meaning as in Eq. 3, $i_{deact,c}$ and $i_{deacts2}$ are the initial amplitudes, and $\tau_{deact,c}$ and $\tau_{deact,s}$ are the time constants of the channel and the unspecific current components, respectively. The amplitude of the unspecific current component was usually small (in the range of a few pA) compared to the up to 100-fold larger channel current component (see Fig. 7, *C–F*). The activation and deactivation time constants of the unspecific component amounted to ~300 ms (7). The unspecific current component is evident only in Fig. 7 *C* as a second slow component of activation or deactivation, where the noisy channel component is small and fast-deactivating.

Fig. 7, *C–F*, shows representative current traces used for the analysis. The curve fits demonstrate that both the rate of current activation and deactivation depended critically on the

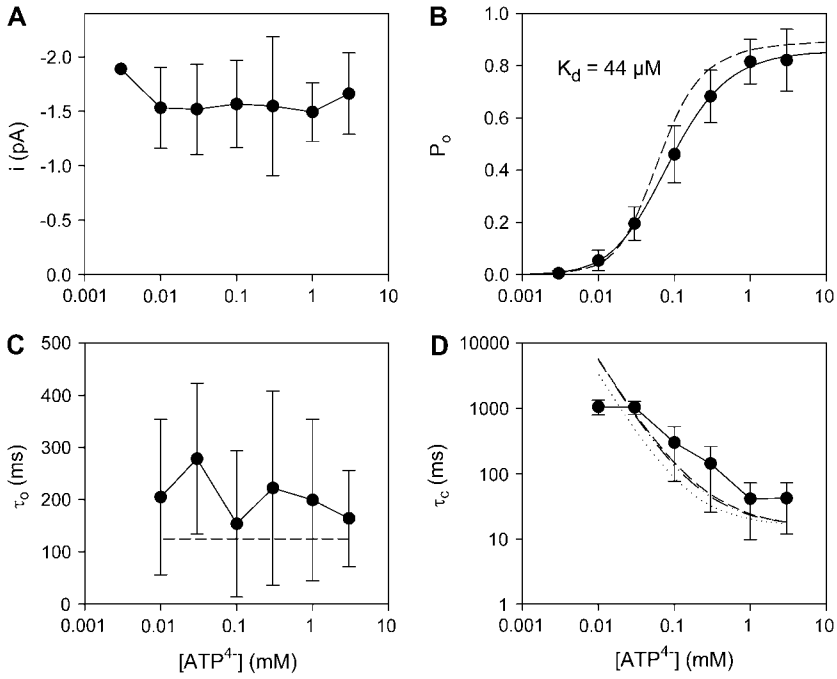

FIGURE 5 P2X$_7$ receptor single-channel currents in K^+-containing extracellular solution. Shown is the [ATP^{4-}] dependence of single-channel conductance (*A*), open probability (*B*), mean open (*C*) and mean closed times (*D*). Data in *B* were fitted according to Eq. 2. Dashed lines in *B* and *C* are calculated according to our model (see Discussion). In *D*, dashed and dotted lines show the [ATP^{4-}] dependence of the three mean closed times predicted by the model. $N = 3$–6; K^+ pipette solution, $V_h = -120$ mV.

cation species present during ATP^{4-} application and washout, respectively. ATP^{4-}-induced current activation was fast in Na^+-based external solutions (*C* and *D*) and significantly slower in K^+-based external solutions (*E* and *F*). Irrespective of whether Na^+ (*C* and *D*) or K^+ (*E* and *F*) was the principal cation during the initial channel activation, deactivation occurred rapidly or slowly when the washing solution contained Na^+ (*C* and *E*) or K^+ (*D* and *F*), respectively, as the principal cation.

A statistical and quantitative evaluation of the data is given in Fig. 8. Successive substitution of extracellular Na^+ by K^+ did not significantly change the single-channel current amplitude (Fig. 8 *A*), but increased the averaged patch current (Fig. 8 *B*), which may reflect the increased open probability observed at the single-channel level.

To account for variable levels of channel expression, the hP2X$_7$ receptor-dependent current $I([Na])$, evoked by 0.1 mM ATP^{4-} in bathing solutions with a certain concentration of Na^+, was normalized to the current $I([0])$ evoked in a solution containing no Na^+, but 100 mM K^+. The dose-response curve for Na^+ was fitted (Fig. 8 *B*) by the Hill equation:

$$I_{rel}(Na^+) = \frac{I([Na])}{I([0])} = \frac{1 - I_{rel,min}}{1 + \left(\frac{[Na]}{10^{-\log EC_{50}}}\right)^n} + I_{rel,min}, \qquad (5)$$

where $I_{rel,\,min}$ is the minimal relative hP2X$_7$ receptor current evoked in solution containing 100 mM Na^+ and no K^+, EC_{50} is the Na^+ concentration (in M) for half maximal inhibition of the Na^+-dependent current, and n is the Hill slope. At a holding potential of -120 mV, the logEC_{50} was approximated to -2.24 ± 0.03 and n to 1.2 ± 0.1 (mean ± SE for all the approximated parameters). At a V_h of -50 mV, a significantly lower logEC_{50} of -1.94 ± 0.06 was obtained, indicating that the effect of Na^+ is voltage-dependent. The coefficient n, however, remained virtually unchanged by the holding potential (1.1 ± 0.2 at -50 mV).

Similarly, the mean open times τ_o (Fig. 8 *C*) and the time constant of ATP^{4-}-dependent activation τ_{act} of mean ensemble currents (Fig. 8 *E*) were strongly dependent on the extracellular Na^+ concentration; this dependency was also approximated in a manner similar to Eq. 5:

$$\tau(Na^+) = \frac{\tau_{max} - \tau_{min}}{1 + \left(\frac{[Na]}{10^{-\log EC_{50}}}\right)^n} + \tau_{min}. \qquad (6)$$

Neither the logEC_{50} values -2.45 ± 0.02 for τ_o and -2.23 ± 0.05 for τ_{act}) nor the Hill slopes (1.2 ± 0.1 for τ_o and 1.3 ± 0.2 for τ_{act}) were significantly different from the logEC_{50} values determined for the Na^+ concentration dependence of the relative currents (all measured at -120 mV). The mean closed times (Fig. 8 *D*), as well as the deactivation time course (Fig. 8 *F*), were unaffected by the Na^+ concentration during the current activation. The deactivation time course, however, was significantly decelerated if the extracellular solution applied during ATP^{4-} washout contained K^+ instead of Na^+ (Fig. 8 *F*).

DISCUSSION

Permeation behavior of single P2X$_7$ receptors

In this work, the ability of the P2X$_7$ receptor channel to discriminate between cations of increasing size was investigated.

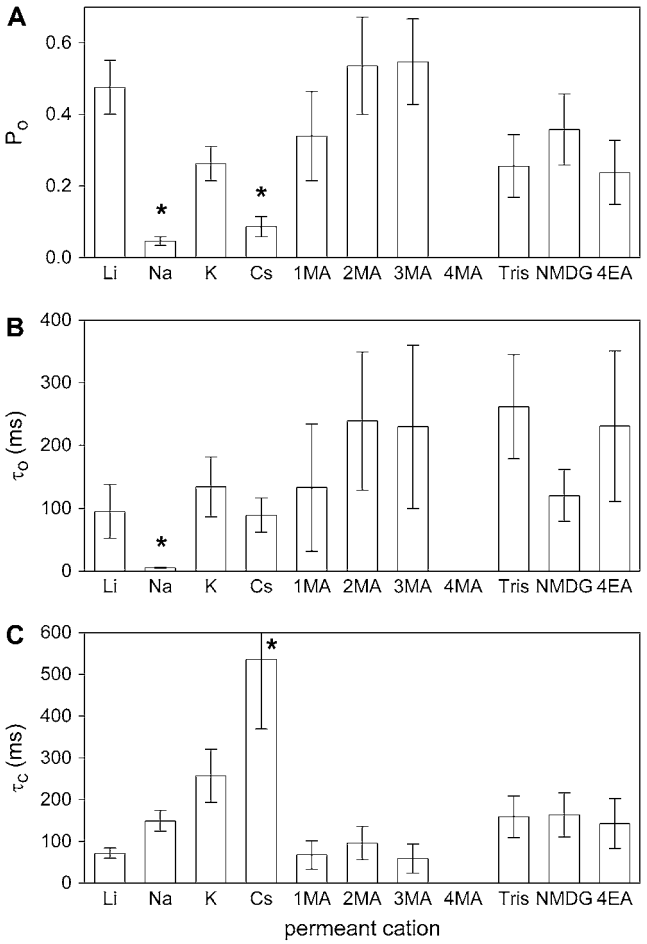

FIGURE 6 Influence of extracellular cation species on kinetics of $hP2X_7$ receptor-operated single-channel currents. Statistics of open probability (*A*) (determined as shown in Fig. 3), mean open time (*B*), and mean closed time (*C*) (both calculated as demonstrated in Fig. 4). mean ± SE, $N = 3$–12; K^+ pipette solution, $V_h = -140$ mV, $[ATP^{4-}] = 0.1$ mM. Columns labeled with different signs are significantly different.

Voltage ramps were applied to single $P2X_7$ channels to measure the dependence of the conductance and the reversal potential of $P2X_7$ receptor-dependent currents on the species of the extracellular cation. We found that the $P2X_7$ channel discriminates poorly between the alkali cations Na^+, Li^+, K^+, and Cs^+, ranging in size from 1.20 to 3.38 Å. The reversal potentials of these alkali cations were not significantly different, suggesting that Na^+, Li^+, K^+, and Cs^+ have a similar permeability near 0 mV. However, single-channel conductances varied significantly. Based on the bi-ionic channel conductances (Cs^+ intracellularly and different monovalent cations extracellularly), the selectivity sequence is $Na^+ > Cs^+ \approx K^+ > Li^+$, corresponding most closely to Eisenman's sequence VII. This finding suggests that cations interact with a site of intermediate field strength when they permeate through the channel (12). For the $P2X_2$ receptor, a weak field sequence (Eisenman sequence IV) was found based on the bi-ionic current amplitude, with K^+ being more permeant than Na^+ (18). Overall, the permeation characteristics of the $P2X_7$ receptor ion channel are similar to those of $P2X_1$ and $P2X_2$ receptors and even of other ligand-gated channels such as nicotinic acetylcholine receptors and 5-hydroxytryptamine 3 ($5\text{-}HT_3$) receptors (18,19).

When organic cations of increasing size (from ~4.5 to 6.5 Å) were used as extracellular charge carriers, γ and V_{rev} changed significantly and approximately in parallel. Within this size range, the single-channel conductance decreased almost linearly with the effective diameter of the permeating organic cation, indicating a sieving effect of the selectivity filter, the diameter of which was extrapolated to 8.5 Å. A similar minimum diameter of 8 Å of the initial ''nondilated'' pore was obtained from whole-cell recordings of HEK293 cells expressing the rat $P2X_7$ receptor (8). Based on intracellular pH changes caused by the influx of NH_4^+ derivatives, it has been concluded that $1MA^+$ and $2MA^+$, but not $3MA^+$ or triethylammonium$^+$, can permeate native purinergic P2Z receptor channels of human B-lymphocytes (20), which almost certainly represent genuine $P2X_7$ receptors (21). We suggest that the higher sensitivity of the patch-clamp technique for detection of cation fluxes, as compared to pH measurements with fluorescent indicators, accounts for this apparent discrepancy. Very low permeability to large organic cations such as $NMDG^+$, $Tris^+$, $4MA^+$, and $4EA^+$ has been observed previously for $P2X_2$ receptors (18).

The selectivity filter of the $hP2X_7$ receptor seems to discriminate poorly between organic cations of diameters between 6.7 Å ($4MA^+$) and 8.3 Å ($4EA^+$). A similar observation was made by single-channel current recordings of $P2X_2$ receptors and attributed to nonionic interactions of the organic cations with the hydrophobic channel (18). Such hydrophobic interactions may also occur between organic cations and the $P2X_7$ receptor. There are, however, alternative explanations for the poor discriminating capability, such as uncertainties in estimates of the effective diameter of organic cations or the possibility that the selectivity filter behaves as a flexible rather than a rigid concentric ring.

The largest measurable permeant organic cation that we used was TEA^+, with a molecular mass of 130 Da. Attempts to test the somewhat larger cation tetrabutylammonium$^+$ failed because tetrabutylammonium$^+$ quickly disrupted the gigaseal. The 130-Da mass of TEA^+ is far below the 314 Da of the organic cation ethidium$^+$, which was found, using whole-cell measurements, to permeate native P2Z receptors (22) and recombinant $P2X_7$ receptors in several (8,23–30) but not all preparations (14,15,31,32).

In the experiments described here, an increase of neither the single-channel amplitude nor the conductance or reversal potential occurred during prolonged exposure to ATP. Also the single-channel kinetics did not change under these experimental conditions (7). Similar results were found for single-channel recordings of the P2Z receptor expressed in human B lymphocytes (21). Taken together, these findings

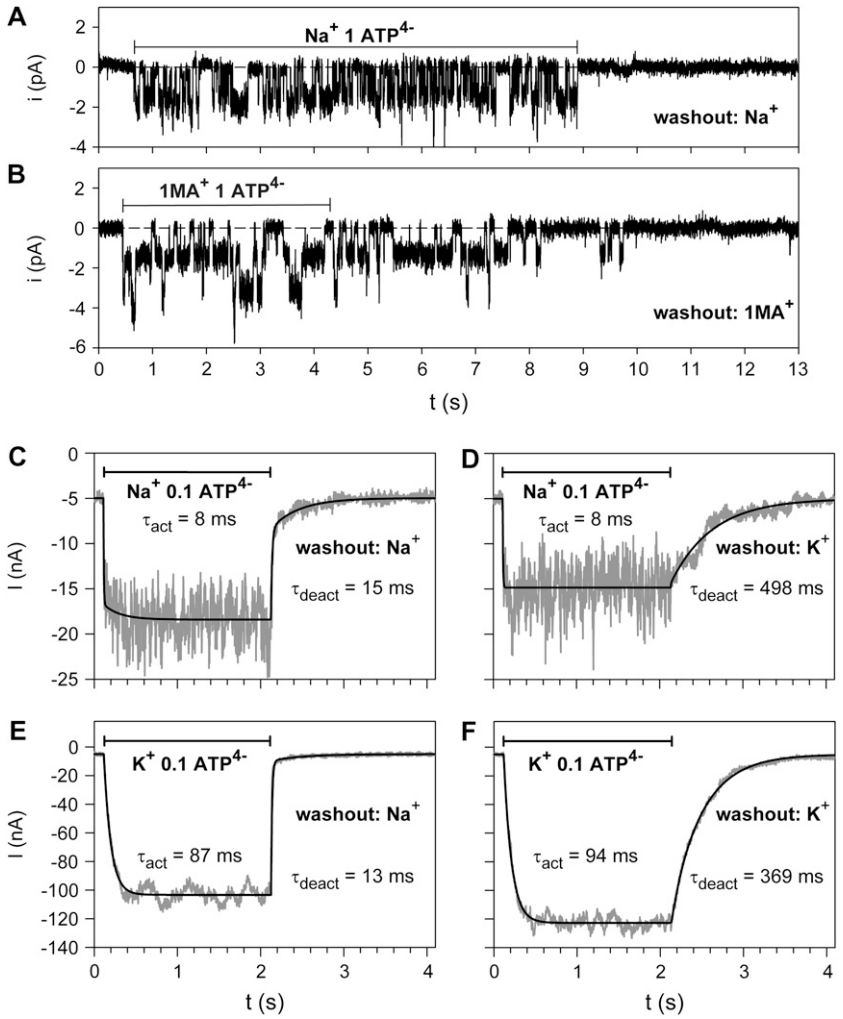

FIGURE 7 Influence of extracellular cation species on activation and deactivation kinetics of hP2X$_7$ receptors. (*A* and *B*) Shown are typical current traces from an apparent four-channel patch demonstrating the different deactivation behavior of single P2X$_7$ receptor channels in extracellular solutions containing (*A*) Na^+ or (*B*) $1MA^+$ as the principal cations. Exposure to 1 mM ATP^{4-} is indicated by the horizontal bar. The leak and nonspecific ATP^{4-}-induced currents have been subtracted. (*C–F*) Effect of extracellular monovalent cations (100 mM Na^+ or K^+) on the activation time course (during ATP^{4-} application) and the deactivation time course (during washout with indicated washing solution) of currents from patches expressing many P2X$_7$ receptors. Horizontal bars indicate the presence of 0.1 mM ATP^{4-}. Labeling by Na^+ or K^+ below the horizontal bars indicates the principal cation present during current activation. The principal cation present during ATP^{4-} washout, Na^+ or K^+, is indicated in the right half of each panel. Each of the current traces in gray was obtained by averaging two typical current traces from the same multichannel patch. The solid black lines represent fits of the activation and deactivation time course according to Eqs. 3 and 4, respectively. The calculated time constants are indicated. The slow component of the current decay in high sodium solution (C and *E*) is due to residual nonspecific ATP^{4-}-activated current that is not related to P2X$_7$ receptor expression.

strongly suggest that ethidium$^+$ uptake during sustained ATP activation does not reflect a dilatation of the genuine pore of the P2X$_7$ receptor, but an opening of a distinct channel secondary to the sustained activation hP2X$_7$ receptor. This secondarily-opened separate channel might be the pannexin hemichannel (6). The intriguing observation that P2X$_2$ and P2X$_4$ receptors also change their ion selectivity in seconds (33,34) could also not be confirmed at the single-channel level (18,35). Altogether, these findings suggest that pore dilation is an epiphenomenon of P2X$_7$ receptor activation.

Extracellular Na^+ favors closure of the P2X$_7$ receptor channel

Substitution of extracellular Na^+ by any other tested alkali or organic cation not only influenced the permeation characteristics of single P2X$_7$ receptor-dependent ion currents, but also drastically changed the kinetic behavior of the P2X$_7$ receptor. In particular, the mean open time, the open probability, and the activation and deactivation time constants increased. This effect can be explained by the existence of a specific Na^+ binding site with a K_d of ~5 mM. Occupancy of this site by Na^+ favors closure of the open P2X$_7$ receptor channel. The Na^+ binding site must be located extracellularly, because substitution or readdition of Na^+ at the extracellular side of the membrane changed the kinetic behavior within milliseconds. In contrast, substitution of intracellular Cs^+ or K^+ by Na^+ did not significantly change the kinetics of single P2X$_7$ receptors (data not shown). Furthermore, the Na^+ binding site must be located within the electrical field of the membrane, since the Na^+ effect turned out to be membrane-voltage-dependent, although only weakly. The weakening of the Na^+ effect at more positive voltages implies that at sufficient positive membrane potentials, a prolongation of the mean open time and an increase of the open probability should occur. This was indeed what we observed. In experiments not shown here, changing V_m from −120 mV to +60 mV in the presence of 0.1 mM ATP^{4-} increased the mean open time from 4 ± 2 ms to 15 ± 4 ms, the open probability from 0.1 ± 0.05 to 0.25± 0.08, the activation time constant from 18 ± 8 ms to 27 ± 10 ms, and the deactivation time constant from 19 ± 6 ms to 35 ± 9 ms.

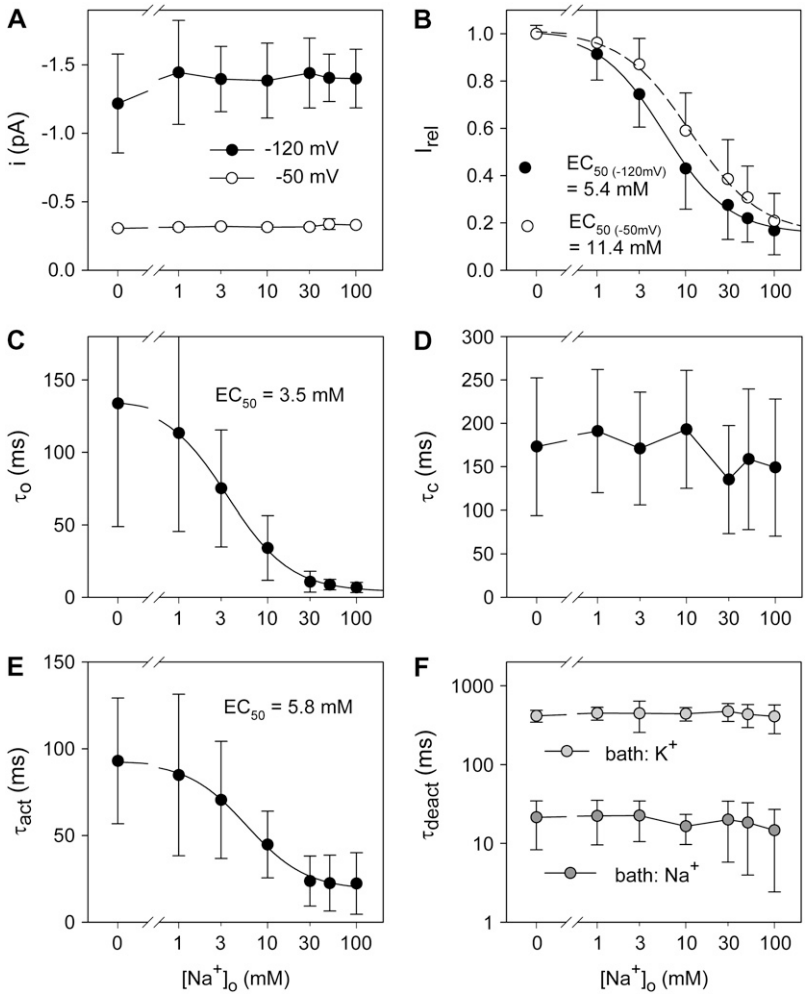

FIGURE 8 Dependence of $P2X_7$ receptor single-channel currents on the extracellular Na^+ concentration. Patches were held at −120 mV in bathing solutions containing 100 mM of either Na^+ or K^+ if not specified otherwise. Singe-channel currents were recorded 1 s after initiating receptor activation by switching to extracellular solutions containing 0.1 mM ATP^{4-} and Na^+ in concentrations as indicated on the abscissa, with $[Na^+]_o + [K^+]_o = 100$ mM. Since the ATP^{4-}-evoked currents were not influenced by preincubation of the patch in bathing solutions with 100 mM Na^+ or K^+, data from otherwise identical conditions were pooled. (*A* and *B*) Influence of activating $[ATP^{4-}]$ and V_h on single-channel conductance and relative open probability at the indicated Na^+ concentration. The relative open probability of the ATP^{4-}-activated channels in the same patch was calculated by comparing the currents (averaged over 1 s) recorded in the absence and presence of extracellular Na^+ (Eq. 5). (*C* and *D*) Dependence of the mean open and closed times, respectively, on the extracellular Na^+ concentration during ATP^{4-}-dependent activation. Superimposed fits in *B*, *C*, and *E* were calculated according to Eqs. 5 and 6. (*E*) Dependence of the activation time course on $[Na^+]_o$ during activation of the current. τ_{act} was calculated according to Eq. 3. (*F*) Influence of $[Na^+]_o$ during activation (as indicated on the abscissa) and deactivation (bath with 100 mM K^+ or Na^+, as indicated) on the deactivation time course. τ_{deact} was calculated according to Eq. 4.

Long openings with a τ_o of ~20 ms, however, were even observed in some patches when $P2X_7$ receptor activity was measured at negative membrane potentials, especially at high $[ATP^{4-}]$ (7). We do not yet have an explanation for this. It is possible that the Na^+ binding site is not stable and is somehow influenced by ATP^{4-}.

The effect of Na^+ substitution on single-channel purinergic receptors has been investigated for heterologously expressed $P2X_2$ receptors (16) and native $P2X_7$-like receptors of airway ciliated cells (36). In both cases, Na^+ removal had no effect on single-channel open times, suggesting that the profound effect of Na^+ on the probability and duration of single-channel opening is specific for $P2X_7$ receptor channels.

Modeling the effect of Na^+ on single $P2X_7$ receptor channel kinetics

In a previous article, we showed that the principal microscopic and macroscopic kinetics of the $P2X_7$ receptor channel can be described by a linear model comprising three closed and one open state (C_1-C_2-C_3-O_4) with the rate constants $k_{12} = 720\ mM^{-1}\ s^{-1}$, $k_{21} = 50\ s^{-1}$, $k_{23} = 360\ mM^{-1}\ s^{-1}$, $k_{32} = 100\ s^{-1}$, $k_{34} = 66\ s^{-1}$, and $k_{43} = 200\ s^{-1}$ (7). As shown here, one obvious effect of Na^+ substitution on microscopic $P2X_7$ receptor channel kinetics is the prolongation of the mean open time (τ_o). Accordingly, to account for the effect of Na^+ replacement, the rate constant k_{43}, which determines τ_o, was decreased from 200 $s^{-1}$to 8 s^{-1}. This reduction of k_{43} increased the predicted parameters τ_o, P_o τ_{act}, and τ_{deact}, which corresponds well with the values determined experimentally. In detail, the calculated mean open time was increased from 5 to 125 ms (see Fig. 8 *C*), the maximal open probability from 0.24 to 0.89 (compare (7) and data of Fig. 5 *B*), the activation time constant from 15 to 81 ms (see Fig. 8 *E*), and the deactivation time constant from 20 to 212 ms (see Fig. 8 *E*). The mean closed times remained unchanged by this modification of the model. The model also comprises three different mean closed times (see Fig. 5 *D*), which are, however, so similar that they could not be separated by our recording and analyzing method. The predicted closed times are within one standard deviation of the experimental data, except for the highest τ_c values at the lowest

ATP^{4-} concentration. This deviation is probably an artifact resulting from our recording system, which does not recognize dwell times longer than 4 s. The P_o (ATP^{4-}) relationship in Na^+-free solution is also approximately described by the model (Fig. 5 *B*). Remarkably, although we only changed the magnitude of the rate constant k_{43} for $hP2X_7$ channel closing, a reduction of the apparent K_d for ATP^{4-} from 251 μM in Na^+-containing extracellular solution (7) to 44 μM in Na^+-free solution was predicted, which is in accordance with the experimental data. Such an apparent increase of a binding site affinity due to an increased efficacy has been described in detail by Colquhoun (37).

Possible physiological relevance of the Na^+-dependent modulation of $hP2X_7$ channel gating

It is well known that substitution of extracellular Na^+ by K^+ or organic cations increases the influx of Ba^{2+}, ethidium$^+$ (22), and Ca^{2+} (38) into P2Z receptor-expressing B lymphocytes. Likewise, extracellular Na^+ removal has been reported to activate secondary divalent-dependent currents in $hP2X_7$ receptor-expressing *Xenopus* oocytes (15), to permeabilize $hP2X_7$ receptor-expressing HEK293 cells for $NMDG^+$ (39), and to increase airway ciliary motility by activating a native $P2X_7$-like receptor (36). These effects were explained by a competition between Na^+ and Ca^{2+} within the permeation pathway (38), an extracellular Na^+ binding site inhibiting pore formation of the $P2X_7$ receptor (39), or a competitive inhibition by Na^+ of the ATP^{4-}-dependent activation of the purinergic receptor (36). According to the effect of extracellular Na^+ on the $P2X_7$ receptor at the single-channel level described here, these macroscopic effects may be explained by the increase of the open probability, which may drastically increase the $P2X_7$ receptor-dependent Ca^{2+} influx, assuming an unchanged Ca^{2+} permeability of the channel pore in Na^+-free extracellular solution. The Ca^{2+} influx might be further augmented by the long channel openings observed under Na^+ free conditions. This may increase the intracellular Ca^{2+} concentration near the inner side of the cell membrane, since the intracellular Ca^{2+} buffers may become saturated if the $hP2X_7$ receptor channel stays continuously open for several hundred milliseconds. The strongly increased $[Ca^{2+}]_i$ may then be responsible for the pore formation (as already suggested by (40)) and the enhanced ciliary motility.

Other intracellular or membrane-delimited signaling pathways leading secondarily to pore formation are possible. In $hP2X_7$ receptor-expressing *Xenopus* oocytes, prolonged ATP^{4-} application leads to a quick change of the reversal potential of whole-cell currents recorded the by two-electrode voltage clamp technique in Na^+- and Ca^{2+}-free extracellular solutions (9) Furthermore, under these experimental conditions, a slow current increase in Na^+-containing Ca^{2+}-free bathing solutions was measured during ATP application. Both effects were not observed under the patch-clamp conditions applied here. Patch clamp measurements could not be performed under Ca^{2+}-free conditions since the patches became unstable. Therefore, we cannot rule out the possibility that Ca^{2+} withdrawal is involved in the effects on whole cell currents.

Under conditions of tissue injury, not only ATP but also K^+ is released from necrotic cells. Furthermore, hypoxic conditions are known to induce the secretion of ATP and K^+ from metabolically malfunctioning cells (2,41,42). In metabolically compromised tissues, a replacement of extracellular Na^+ by K^+ may occur that could enhance the efficacy and potency of ATP^{4-} on $P2X_7$ receptor-expressing cells of the immune and inflammatory system. Furthermore, ATP-mediated cell depolarization (38) increases the driving force for K^+ efflux and lowers the EC_{50} value of Na^+ at the Na^+ binding site to favor channel closing. In this way, K^+ efflux may reinforce the ATP^{4-} effect on $P2X_7$-receptor-expressing cells and even low concentrations of ATP^{4-} may be capable of activating the $P2X_7$ receptor to a substantial extent.

In summary, by single-channel analysis, we have shown here that the cation channel of the $hP2X_7$ receptor does not undergo pore dilatation upon sustained activation. According to our results, the cation pore of $P2X_7$ receptors has conventional fixed permeation properties similar to the pores of other ligand-gated cationic channels. Extracellular Na^+ exerted a drastic effect on single-channel and macroscopic kinetics, which could be explained by an allosterically induced acceleration of channel closing by extracellular Na^+, resulting in a Na^+-dependent decrease of the efficacy of ATP^{4-} to activate the channel. Insights into the precise mechanism by which Na^+ exerts these effects may come from a combination of single-channel recordings and site-directed mutagenesis.

SUPPLEMENTARY MATERIAL

To view all of the supplemental files associated with this article, visit www.biophysj.org.

This work was supported by grants from the Deutsche Forschungsgemeinschaft (Ma1581/12-1 to F.M. and Schm536/6-1 to G.S.) and the Roux-program of the Medical Faculty of Martin Luther University Halle (Roux 5/09, 10/01, and 13/07 to F.M.).

REFERENCES

1. Ferrari, D., C. Pizzirani, E. Adinolfi, R. M. Lemoli, A. Curti, M. Idzko, E. Panther, and F. Di Virgilio. 2006. The $P2X_7$ receptor: a key player in IL-1 processing and release. *J. Immunol.* 176:3877–3883.
2. North, R. A. 2002. Molecular physiology of P2X receptors. *Physiol. Rev.* 82:1013–1067.
3. Khakh, B. S., and H. A. Lester. 1999. Dynamic selectivity filters in ion channels. *Neuron.* 23:653–658.
4. Schilling, W. P., T. Wasylyna, G. R. Dubyak, B. D. Humphreys, and W. G. Sinkins. 1999. Maitoxin and P2Z/$P2X_7$ purinergic receptor stimulation activate a common cytolytic pore. *Am. J. Physiol.* 277: C766–C776.

5. Elliott, J. I., A. Surprenant, F. M. Marelli-Berg, J. C. Cooper, R. L. Cassady-Cain, C. Wooding, K. Linton, D. R. Alexander, and C. F. Higgins. 2005. Membrane phosphatidylserine distribution as a non-apoptotic signalling mechanism in lymphocytes. *Nat. Cell Biol.* 7:808–816.
6. Pelegrin, P., and A. Surprenant. 2006. Pannexin-1 mediates large pore formation and interleukin-1 release by the ATP-gated $P2X_7$ receptor. *EMBO J.* 25:5071–5082.
7. Riedel, T., I. Lozinsky, G. Schmalzing, and F. Markwardt. 2006. Kinetics of $P2X_7$ receptor-operated single-channel currents. *Biophys. J.* 92:2377–2391.
8. Virginio, C., A. MacKenzie, R. A. North, and A. Surprenant. 1999. Kinetics of cell lysis, dye uptake and permeability changes in cells expressing the rat $P2X_7$ receptor. *J. Physiol.* (*Lond.*). 519:335–346.
9. Boldt, W., M. Klapperstück, C. Büttner, S. Sadtler, N. Schmalzing, and F. Markwardt. 2003. $Glu^{496}Ala$ polymorphism of human $P2X_7$ receptor does not affect its electrophysiological phenotype. *Am. J. Physiol.* 284:C749–C756.
10. Neher, E. 1992. Correction for liquid junction potentials in patch clamp experiments. *In* Ion Channels. B. Rudy and L. Iverson, editors. Academic Press, San Diego. 123–131.
11. Schubert, R. 1996. Multiple ligand-ion solutions: a guide for solution preparation and computer program understanding. *J. Vasc. Res.* 33:86–98.
12. Hille, B. 2001. Ion Channels of Excitable Membranes. Sinauer Associates, Sunderland, MA.
13. Colquhoun, D., and A. G. Hawkes. 1977. Relaxation and fluctuations of membrane currents that flow through drug-operated channels. *Proc. R. Soc. Lond. B Biol. Sci.* 199:231–262.
14. Bretschneider, F., M. Klapperstück, M. Löhn, and F. Markwardt. 1995. Nonselective cationic currents elicited by extracellular ATP in human B-lymphocytes. *Pflugers Arch.* 429:691–698.
15. Klapperstück, M., C. Büttner, T. Böhm, G. Schmalzing, and F. Markwardt. 2000. Characteristics of $P2X_7$ receptors from human B lymphocytes expressed in *Xenopus* oocytes. *Biochim. Biophys. Acta.* 1467:444–456.
16. Ding, S. H., and F. Sachs. 1999. Single channel properties of $P2X_2$ purinoceptors. *J. Gen. Physiol.* 113:695–719.
17. Egan, T. M., and B. S. Khakh. 2004. Contribution of calcium ions to P2X channel responses. *J. Neurosci.* 24:3413–3420.
18. Ding, S., and F. Sachs. 1999. Ion permeation and block of $P2X_2$ purinoceptors: single channel recordings. *J. Membr. Biol.* 172:215–223.
19. Evans, R. J., C. Lewis, C. Virginio, K. Lundstrom, G. Buell, A. Surprenant, and R. A. North. 1996. Ionic permeability of, and divalent cation effects on, two ATP-gated cation channels (P2X receptors) expressed in mammalian cells. *J. Physiol.* (*Lond.*). 497:413–422.
20. Chen, J. R., G. P. Jamieson, and J. S. Wiley. 1994. Extracellular ATP increases NH_4^+ permeability in human lymphocytes by opening a P2Z purinoceptor operated ion channel. *Biochem. Biophys. Res. Commun.* 202:1511–1516.
21. Markwardt, F., M. Löhn, T. Böhm, and M. Klapperstück. 1997. Purinoceptor-operated cationic channels in human B lymphocytes. *J. Physiol.* (*Lond.*). 498:143–151.
22. Wiley, J. S., R. Chen, and G. P. Jamieson. 1993. The ATP^{4-} receptor-operated channel (P_2Z class) of human lymphocytes allows Ba^{2+} and $ethidium^+$ uptake: inhibition of fluxes by suramin. *Arch. Biochem. Biophys.* 305:54–60.
23. Cockcroft, S., and B. D. Gomperts. 1979. ATP induces nucleotide permeability in rat mast cells. *Nature.* 279:541–542.
24. Steinberg, T. H., A. S. Newman, J. A. Swanson, and S. C. Silverstein. 1987. ATP^{4-} permeabilizes the plasma membrane of mouse macrophages to fluorescent dyes. *J. Biol. Chem.* 262:8884–8888.
25. Nuttle, L. C., and G. R. Dubyak. 1994. Differential activation of cation channels and non-selective pores by macrophage P_{2z} purinergic receptors expressed in *Xenopus* oocytes. *J. Biol. Chem.* 269:13988–13996.
26. Surprenant, A., F. Rassendren, E. Kawashima, R. A. North, and G. Buell. 1996. The cytolytic P_{2Z} receptor for extracellular ATP identified as a P_{2X} receptor ($P2X_7$). *Science.* 272:735–738.
27. Rassendren, F., G. N. Buell, C. Virginio, G. Collo, R. A. North, and A. Surprenant. 1997. The permeabilizing ATP receptor, $P2X_7$. Cloning and expression of a human cDNA. *J. Biol. Chem.* 272:5482–5486.
28. Chessell, I. P., A. D. Michel, and P. P. A. Humphrey. 1997. Properties of the pore-forming $P2X_7$ purinoceptor in mouse NTW8 microglial cells. *Br. J. Pharmacol.* 121:1429–1437.
29. Chessell, I. P., C. B. A. Grahames, A. D. Michel, and P. P. A. Humphrey. 2001. Dynamics of $P2X_7$ receptor pore dilation: pharmacological and functional consequences. *Drug Dev. Res.* 53:60–65.
30. Smart, M. L., B. Gu, R. G. Panchal, J. Wiley, B. Cromer, D. A. Williams, and S. Petrou. 2003. $P2X_7$ receptor cell surface expression and cytolytic pore formation are regulated by a distal C-terminal region. *J. Biol. Chem.* 278:8853–8860.
31. Petrou, S., M. Ugur, R. M. Drummond, J. J. Singer, and J. V. Walsh. 1997. $P2X_7$ purinoceptor expression in *Xenopus* oocytes is not sufficient to produce a pore-forming P2Z-like phenotype. *FEBS Lett.* 411: 339–345.
32. Amstrup, J., and I. Novak. 2003. $P2X_7$ receptor activates extracellular signal-regulated kinases ERK1 and ERK2 independently of Ca^{2+} influx. *Biochem. J.* 374:51–61.
33. Virginio, C., A. MacKenzie, F. A. Rassendren, R. A. North, and A. Surprenant. 1999. Pore dilation of neuronal P2X receptor channels. *Nat. Neurosci.* 2:315–321.
34. Khakh, B. S., X. R. Bao, C. Labarca, and H. A. Lester. 1999. Neuronal P2X transmitter-gated cation channels change their ion selectivity in seconds. *Nat. Neurosci.* 2:322–350.
35. Negulyaev, Y. A., and F. Markwardt. 2000. Block by extracellular Mg^{2+} of single human purinergic $P2X_4$ receptor channels expressed in human embryonic kidney cells. *Neurosci. Lett.* 279:165–168.
36. Ma, W. Y., A. Korngreen, N. Uzlaner, Z. Priel, and S. D. Silberberg. 1999. Extracellular sodium regulates airway ciliary motility by inhibiting a P2X receptor. *Nature.* 400:894–897.
37. Colquhoun, D. 1998. Binding, gating, affinity and efficacy: the interpretation of structure-activity relationships for agonists and of the effects of mutating receptors. *Br. J. Pharmacol.* 125:924–947.
38. Löhn, M., M. Klapperstück, D. Riemann, and F. Markwardt. 2001. Sodium block and depolarization diminish P2Z-dependent Ca^{2+} entry in human B lymphocytes. *Cell Calcium.* 29:395–408.
39. Jiang, L. H., F. Rassendren, A. MacKenzie, Y. H. Zhang, A. Surprenant, and R. A. North. 2005. N-methyl-D-glucamine and propidium dyes utilize different permeation pathways at rat $P2X_7$ receptors. *Am. J. Physiol.* 289:C1295–C1302.
40. Faria, R. X., F. P. DeFarias, and L. A. Alves. 2005. Are second messengers crucial for opening the pore associated with $P2X_7$ receptor? *Am. J. Physiol.* 288:C260–C271.
41. Di Virgilio, F., D. Ferrari, M. Idzko, E. Panther, J. Norgauer, A. La Sala, and G. Girolomoni. 2003. Extracellular ATP, P2 receptors, and inflammation. *Drug Dev. Res.* 59:171–174.
42. Lim, R. K. S. 1970. Pain. *Annu. Rev. Physiol.* 32:269–288.